

**Effect of nanometer-sized grains on the superhardness of *c*-BC<sub>5</sub>: A first-principles study**

R. F. Zhang\* and S. Veprek

*Department of Chemistry, Technical University Munich, Lichtenbergstr. 4, D-85747 Munich, Germany*

A. S. Argon

*Department of Mechanical Engineering, Massachusetts Institute of Technology, 77 Massachusetts Avenue, Cambridge, Massachusetts 02139, USA*

(Received 9 October 2009; published 2 December 2009)

Using *ab initio* density-functional theory to calculate the anisotropic ideal strengths and electronic structure of *c*-BC<sub>5</sub> with different distribution of boron in the diamond lattice we show that the recently reported load-invariant hardness of 71 GPa cannot be explained by the relatively low intrinsic shear strength of this material, but it is, in agreement with many reports on nanosize effect, extrinsically enhanced by the small crystallites size of 10–15 nm of the samples. It is further shown that random distribution of boron atoms within the diamond lattice results in higher strength than in heterostructures consisting of repetitive stacking of one B and five C layers along the  $\langle 111 \rangle$  direction, which were used by other researchers in their modeling of *c*-BC<sub>5</sub> solid solution

DOI: [10.1103/PhysRevB.80.233401](https://doi.org/10.1103/PhysRevB.80.233401)

PACS number(s): 73.22.-f, 62.25.-g, 31.15.A-, 62.20.Qp

Intrinsically superhard ( $H \geq 40$  GPa) and ultrahard ( $H \geq 80$  GPa) materials attain high hardness through their crystal structure and strong covalent bonds, whereas extrinsically superhard and ultrahard materials reach such hardness through their nanostructure.<sup>1</sup> For example, nanocomposites consisting of cubic (*c*-) and wurtzite (*w*-) BN reach load-invariant hardness of 85 GPa (Ref. 2) at the “strongest size” of 14 nm grains, where the strengthening due to stifled dislocation activity inside grains with decreasing crystallite size becomes replaced by increasing grain boundary shear.<sup>3,4</sup> The maximum hardness enhancement of about two can be achieved by this so-called Hall-Petch effect<sup>4</sup> in many nanostructured materials.<sup>5</sup> Much higher enhancement by a factor of 5 or more can be achieved in ceramic nanocomposites consisting of 3–4 nm size nanocrystals of a hard transition metal nitride joined together by about one monolayer thick, strengthened Si<sub>3</sub>N<sub>4</sub> like interfaces.<sup>6</sup> Hardness of more than 100 GPa has been reported experimentally<sup>6</sup> and explained mechanistically.<sup>7</sup>

Recent search for intrinsically superhard materials has concentrated on those with high elastic moduli (or “low compressibility”). However, elastic moduli describe only the reversible response of a material to small strain near equilibrium whereas plastic deformation at the atomic level occurs by permanent large shear strain, where instabilities of electronic structure and concomitant structural transformation to a softer phase may often occur, as shown, e.g., for *c*-C<sub>3</sub>N<sub>4</sub> (Ref. 8) and ReB<sub>2</sub>.<sup>9</sup> For these reasons, the ideal shear strength is a more relevant indicator for assessing the source of ultimate strength and hardness of a material.<sup>8–11</sup> Using *ab initio* density-functional theory (DFT) we show here that the recently reported high hardness of *c*-BC<sub>5</sub> of 71 GPa (Ref. 12 and 13) is not likely an intrinsic property but it is due to an enhancement resulting from its nanostructure in a manner similar to that reported for the *c*- and *w*-BN nanocomposites<sup>2</sup> and other similar nanostructured materials.<sup>5</sup> Furthermore, we show the importance of random dispersion of B atoms in the BC<sub>5</sub> solid solution, using a sufficiently large cell for physically meaningful calculations because the strength of the het-

erostructure, proposed in Ref. 12, is significantly lower than that of *c*-BC<sub>5</sub> with random distribution of boron atoms in the diamond lattice.

Boron doped diamond attracted much interest because of its high hardness, high chemical stability, and superconductivity with relatively high transition temperature.<sup>12–17</sup> Solozhenko *et al.* reported that the *c*-BC<sub>5</sub> solid solution, synthesized at a pressure of 24 GPa and temperature of 2200 K, has load-invariant hardness of about 71 GPa, with elevated fracture toughness of 9.5 MPa m<sup>0.5</sup> and high thermal stability up to 1900 K.<sup>13</sup> Calandra *et al.*<sup>12</sup> studied, by means of *ab initio* DFT, the superconductivity of *c*-BC<sub>5</sub> using a supercell consisting of six atoms in which one carbon atom has been replaced by boron. After volume and force optimization, they found an average atomic volume of 5.96 Å<sup>3</sup>, which is about 5.2% larger than that of diamond of 5.67 Å<sup>3</sup>, and slightly lower than the experimental value of 6.00 Å<sup>3</sup>.<sup>12,13</sup> Because of the periodic boundary conditions used in their *ab initio* DFT calculations, the structure model used by Calandra *et al.* corresponds to a heterostructure of five layers of carbon and one layer of boron atoms stacked periodically along the  $\langle 111 \rangle$  direction, as shown in Fig. 1 for the equilibrium structure at zero strain. However, such a model is in conflict with the experimentally reported Raman spectrum of *c*-BC<sub>5</sub> which is similar to that of *B*-doped diamond with a random distribution of 1–2 at. % of boron atoms.<sup>13</sup>

Our first-principles calculations of stress-strain response and electronic properties were performed using density functional theory within the generalized gradient approximation as implemented in the Vienna *ab initio* simulation package.<sup>18</sup> The electron-ion interaction is described by the projector augmented wave scheme.<sup>19</sup> The method of the calculation of the stress-strain dependence has been described and carefully verified earlier.<sup>20,21</sup>

Here, we first study the *c*-BC<sub>5</sub> heterostructure proposed by Calandra *et al.* and shown in Fig. 1. Evidently, the ideal shear strength of the (111)[11 $\bar{2}$ ] slip system of about 18.5 GPa is much lower than the lowest value of *c*-BN (58 GPa)

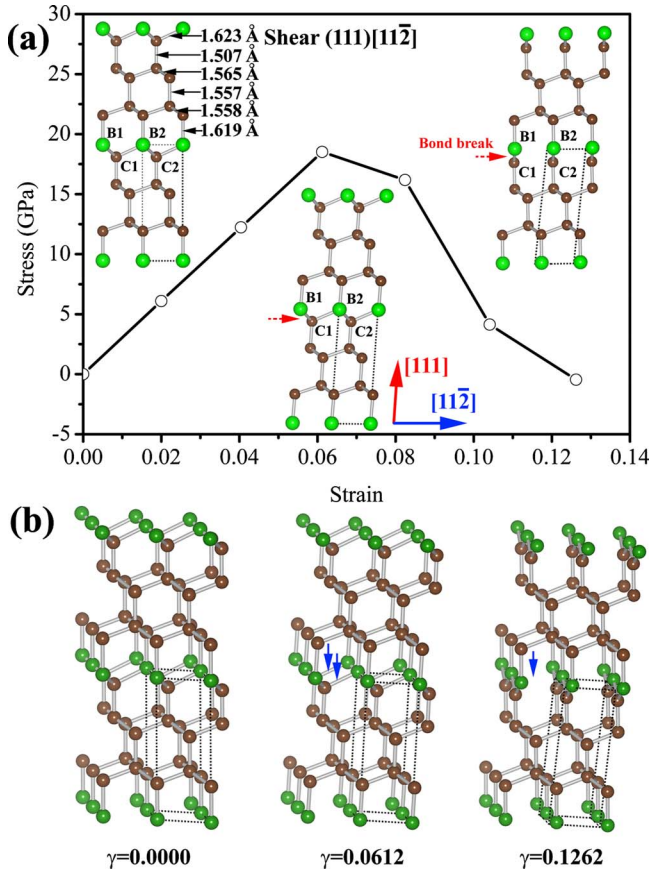


FIG. 1. (Color online) (a) Calculated stress-strain relationship for  $BC_5$  heterostructure corresponding to the model of Calandra *et al.*, (Ref. 12) and the projection of the structure in direction perpendicular to shear in the easiest  $(111)[\bar{1}\bar{1}\bar{2}]$  slip system. The shear occurs around boron layers marked by red/gray dashed arrows. (b): Perspective view of the structures shown in (a) for strains as indicated. The blue/dark solid arrows show the breaking C-B bonds.

and of  $w$ -BN (62 GPa).<sup>21</sup> Because of the difference in electronegativity of carbon (2.5) and boron (2.0),<sup>22</sup> the boron layers are positively charged. Such charged layers reduce the ideal strength of the heterostructures, compared with a homogenous solid solution of B in the diamond lattice. They

would also result in Friedel oscillations of valence charge density as found in heterostructures consisting of one monolayer  $SiN_x$  and 2–3 nm TiN.<sup>23</sup> In the present case, only a small indication of such oscillations of bond length is discernable in Fig. 1(a) because the slab of five layers of C atoms is too thin and the bonding of the boron atoms is asymmetric in the sense that in one direction each B atom is bonded to one C atom at a distance of 1.619 Å but in the other direction two B atoms share one C atom at a bond distance of 1.623 Å. The lengths of the C-C bonds oscillate around an average value of 1.547 Å which is slightly larger than the C-C bond in diamond of 1.544 Å.<sup>22</sup>

To show the atomistic mechanism of ideal shear along the weakest slip system, the projection of the structure perpendicular to the shear direction at strain 0.0612, corresponding to the maximum of the stress-strain curve, is shown in the middle of Fig. 1(a), and at a plastic shear strain of about 0.1262, corresponding to the unloaded state at zero stress, after the shear step. This is shown on the right hand side on Fig. 1(a). We note that the shear occurs within the weakest B-C-B bonds in the so-called “glide set” of  $(111)$  planes between the boron layer and carbon layer next to it, by breaking B-C bonds (see blue/dark solid arrows) and “flip-over” of the B-C-B bonds (see red/gray dashed arrows). After this shear step, the boron atoms remain threefold coordinated to carbon, across the shear plane as seen from the perspective view in Fig. 1(b). The critical shear strain of 0.0612 is relatively small as compared to many other materials. The values of calculated anisotropic ideal strengths in tension in several crystallographic directions and in shear in several slip systems are also summarized in Table I for the heterostructures as well as for the random solid solutions to be discussed next.

In order to model the effect of randomly dispersed boron in the diamond lattice we use a larger cell. To compromise between a too long computing time for a large cell and sufficiently randomized distribution of boron atoms in too small a cell, we used a supercell with a total of 24 atoms. There are many possibilities for distributing boron atoms to be dispersed randomly yet avoiding clustering, i.e., meeting the conditions that all have only carbon as nearest neighbors, in agreement with the Raman spectra that is dominated by signals from B-C bonds with only minor signal from B-B

TABLE I. Calculated anisotropic ideal strengths (all in GPa) for different  $BC_5$  phases,  $c$ -BN, and diamond.

Deformation	Relevant $BC_5$ phases					
	$BC_5$ heterostructures	BC5-I	BC5-II	BC5-III	$c$ -BN	diamond
$\langle 111 \rangle$	69.8	60.3	43.3	47.5	55.3	81.2
$\langle 11\bar{2} \rangle$	48.9	68.7	40.6	42.2	60.3	89.3
$\langle 1\bar{1}0 \rangle$	81.6	42.9	77.3	77.5	84.1	114.6
$(111)[\bar{1}\bar{1}\bar{2}]$	18.5	52.6	47.1	53.6	58.3	86.8
$(111)[\bar{1}\bar{1}2]$	85.7	50.2	39.3	42.5	116.4	162.7
$(111)[1\bar{1}0]$	26.1	43.6	36.8	50.9	68.2	101.2
$(111)[\bar{1}10]$	26.1	48.5	49.9	50.9	68.2	101.2

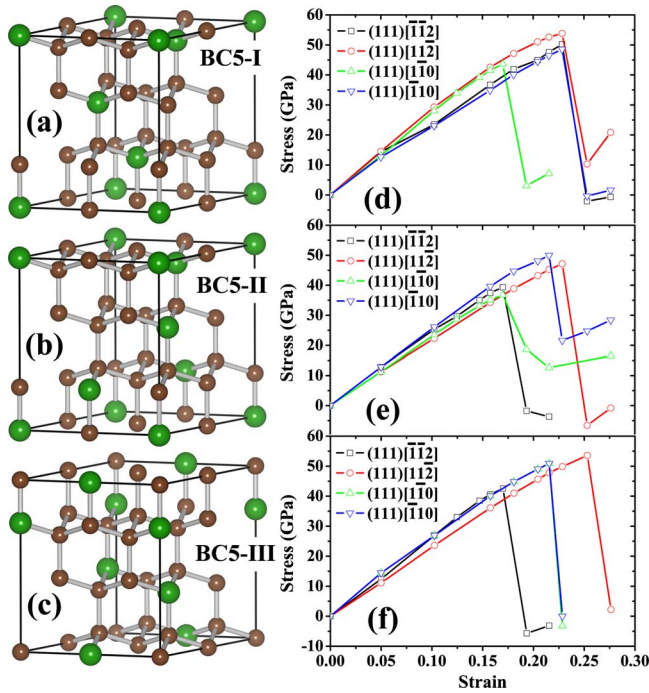


FIG. 2. (Color online) The structural models of (a)  $c$ -BC<sub>5</sub>-I, (b)  $c$ -BC<sub>5</sub>-II, and (c)  $c$ -BC<sub>5</sub>-III, respectively, and their corresponding shear stress-strain curves of (d)  $c$ -BC<sub>5</sub>-I, (e)  $c$ -BC<sub>5</sub>-II, and (f)  $c$ -BC<sub>5</sub>-III, respectively.

bonds.<sup>13</sup> The three choices, that were used, are shown in Figs. 2(a)–2(c) and marked as BC5-I, -II, and -III. Because the calculated ideal shear strengths of all three configurations agree within about 10% and are significantly larger than those of the heterostructures (Fig. 1 and Table I), these three structures are considered sufficient to illustrate the different behavior of  $c$ -BC<sub>5</sub> with random distribution of boron atoms as compared with the heterostructure.

The calculated atomic volumes of the modeled BC5-I, -II, and -III structures of 6.03 Å<sup>3</sup>/atom, 6.028 Å<sup>3</sup>/atom, and 6.026 Å<sup>3</sup>/atom, respectively, agree within ≤0.5% with the experimental value of 6.00 Å<sup>3</sup>.<sup>13</sup> Although the cell shapes of the three BC<sub>5</sub> structures are, after full relaxation, slightly distorted by <5% due to the asymmetric boron distribution, this does not influence significantly the results. Figures 2(d)–2(f) show the calculated shear stress-strain curves on the so-called “glide set” of (111) slip planes which are the weakest in the diamond cubic lattice. The computed ideal strengths are summarized in Table I. The lowest ideal shear strengths of the three  $c$ -BC<sub>5</sub> samples with random B distribution are between 36.8 to 43.6 GPa. This is lower than the lowest shear strengths of  $c$ -BN (58 GPa) and of diamond (87 GPa), but significantly higher than that of the  $c$ -BC<sub>5</sub> heterostructures of 18.5 GPa, and of typical hard materials such as fcc-TiN (29.2 GPa), hcp-Si<sub>3</sub>N<sub>4</sub> (19 GPa) (Ref. 20) and others.

Because of the large concentration of boron in  $c$ -BC<sub>5</sub>, and because the state of boron into the lattice is not well-known, the substantial size misfit between B and C atoms, the statistic of filling volume randomly by spheres, and the appearance of weak signal from B-B bonds in Raman spectrum, we

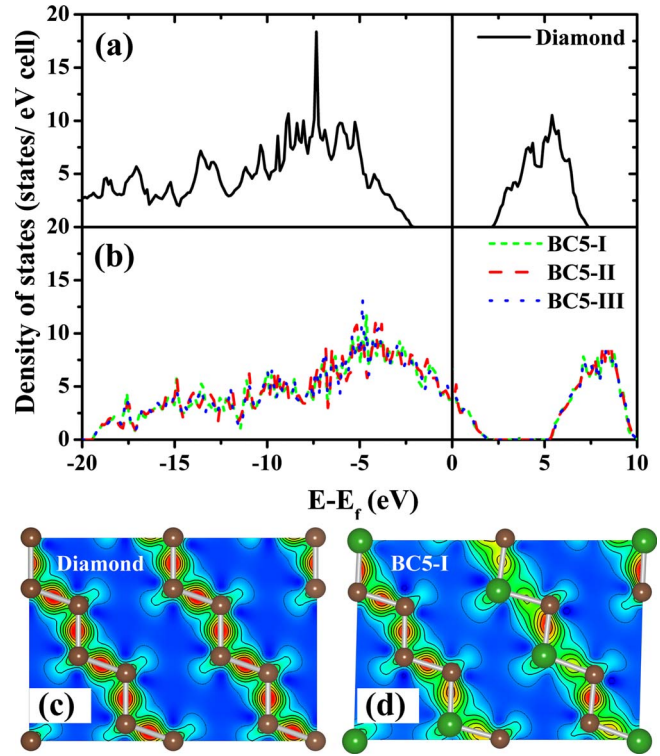


FIG. 3. (Color online) Electronic density of state for (a) Diamond and (b)  $c$ -BC<sub>5</sub> solution phases, and valence charge-density difference of (c) diamond and (d)  $c$ -BC<sub>5</sub>-I. The thick solid and thin dotted contours represent positive and negative value, respectively.

also considered the effect of clustering by conducting the calculations for a cell with B-B dimmers. As expected, the clustering of boron decreases the shear strength of  $c$ -BC<sub>5</sub> below 30 GPa.

In order to obtain deeper insight into the physical origin of the mechanical strength of  $c$ -BC<sub>5</sub> structures, their density of states (DOS) and charge-density difference (CDD), defined as the difference between the calculated total charge density of the crystal minus those of neutral atoms at the given lattice sites, are shown in Fig. 3 in comparison with diamond. Positive and negative values mean a higher and lower valence charge density, respectively. It is seen that all  $c$ -BC<sub>5</sub> phases are metallic because of nonzero DOS values at the Fermi level [Fig. 3(b)]. The CDD maps of diamond and of the  $c$ -BC<sub>5</sub>-I are shown in Figs. 3(c) and 3(d), respectively. Clearly, the weaker, polar B-C bonds is limiting the intrinsic strength of this material when compared to the strong, non-polar C-C bonds in BC<sub>5</sub>, the latter being also somewhat weaker than those in diamond. This explains why  $c$ -BC<sub>5</sub> with randomly distributed boron atoms are weaker than diamond.

The calculated ideal shear strengths of  $c$ -BC<sub>5</sub> with random distribution of boron are lower than those of  $c$ -BN but higher than those of TiN, suggesting that this material is likely to be harder than TiN and other conventional hard materials, but unlikely to be intrinsically harder than  $c$ -BN. Therefore an explanation is needed for the high hardness of about 71 GPa reported by Solozhenko *et al.*<sup>13</sup> During the synthesis, the  $c$ -BC<sub>5</sub> samples were quenched from the high temperature to ambient yielding nanocrystalline material



with average grain size of 10–15 nm,<sup>13</sup> which is in the range where Dubrovinskaia *et al.* reported hardness maximum for *c*-BN and *c*- and *w*-BN nanocomposites.<sup>2</sup> Therefore we suggest that the very high hardness reported by Solozhenko *et al.* is due to a combination of relatively high intrinsic strength of this material, which is however less than that of *c*-BN, and its enhancement by the small size of the nanocrystals. This suggestion is supported by the fact that in all nanocrystalline materials studied so far, hardness maximum has been found for crystallite size in the range of about 10–20 nm, arising from the concurrence of strengthening due to decreasing dislocation activity inside grains and softening due to increasing grain boundary shear with decreasing crystallite size.<sup>3–5</sup>

In summary we have shown that the *c*-BC<sub>5</sub> “heterostructures,” which were investigated by Calandra *et al.*, cannot be used to model *c*-BC<sub>5</sub> solid solution due to the significant weakening of B-C bonds adjacent to the boron layers. The *c*-BC<sub>5</sub> solid solution with a nearly random distribution of boron atoms shows much higher ideal shear strengths, thus suggesting a higher hardness than those of the *c*-BC<sub>5</sub> hetero-

structures and of TiN and other conventional hard materials. However, because the ideal shear strengths of all three *c*-BC<sub>5</sub> random structures studied here are lower than that of *c*-BN, the very high hardness of about 71 GPa reported by Solozhenko *et al.* is probably due to the enhancement by the small crystallite size. Therefore we suggest to study either the intrinsic hardness of large single *c*-BC<sub>5</sub> crystals or the dependence of the load-invariant hardness of polycrystalline *c*-BC<sub>5</sub> as function of the crystallite size in a similar manner as it has been done for the *c*- and *w*-BN nanocomposites by Dubrovinskaia *et al.*<sup>2</sup>

This work has been supported by the German Research Foundation (DFG) and by the European Commission within the project NoE EXCELL under Contract No 5157032. The research of A.S.A. at MIT is presently supported by the Mechanical Engineering Department at MIT. We would like to thank G. Kresse for valuable advice for the application of VASP. We also gratefully acknowledge the Leibniz computer center (LRZ).

---

\*Corresponding author. FAX: +49 89 2891 3626; ruifeng.zhang@lrz.tum.de

<sup>1</sup>S. Veprek, *J. Vac. Sci. Technol. A* **17**, 2401 (1999).

<sup>2</sup>N. Dubrovinskaia, V. L. Solozhenko, N. Miyajima, V. Dmitriev, O. O. Kurakevich, and L. Dubrovinsky, *Appl. Phys. Lett.* **90**, 101912 (2007).

<sup>3</sup>A. S. Argon and S. Yip, *Philos. Mag. Lett.* **86**, 713 (2006).

<sup>4</sup>A. S. Argon, *Strengthening Mechanisms in Crystal Plasticity* (Oxford University Press, Oxford, 2008).

<sup>5</sup>R. W. Siegel and G. E. Fougere, *Nanostruct. Mater.* **6**, 205 (1995).

<sup>6</sup>S. Veprek, M. G. J. Veprek-Heijman, P. Karvanova, and J. Prochazka, *Thin Solid Films* **476**, 1 (2005).

<sup>7</sup>S. Veprek, A. S. Argon, and R. F. Zhang, *Philos. Mag. Lett.* **87**, 955 (2007).

<sup>8</sup>Y. Zhang, H. Sun, and C. Chen, *Phys. Rev. B* **73**, 064109 (2006).

<sup>9</sup>S. Veprek, A. S. Argon, and R. F. Zhang, *Philos. Mag.* (to be published).

<sup>10</sup>R. F. Zhang, S. H. Sheng, and S. Veprek, *Appl. Phys. Lett.* **94**, 121903 (2009).

<sup>11</sup>J. Yang, H. Sun, and C. F. Chen, *J. Am. Chem. Soc.* **130**, 7200 (2008).

<sup>12</sup>M. Calandra and F. Mauri, *Phys. Rev. Lett.* **101**, 016401 (2008).

<sup>13</sup>V. L. Solozhenko, O. O. Kurakevych, D. Andrault, Y. Le Godec, and M. Mezouar, *Phys. Rev. Lett.* **102**, 015506 (2009).

<sup>14</sup>E. A. Ekimov, V. A. Sidorov, E. D. Bauer, N. N. Mel'nik, N. J. Curro, J. D. Thompson, and S. M. Stishov, *Nature (London)* **428**, 542 (2004).

<sup>15</sup>X. Blase, Ch. Adessi, and D. Connétable, *Phys. Rev. Lett.* **93**, 237004 (2004).

<sup>16</sup>E. Bustarret, J. Kacmarcik, C. Marcenat, E. Gheeraert, C. Cytermann, J. Marcus, and T. Klein, *Phys. Rev. Lett.* **93**, 237005 (2004).

<sup>17</sup>T. Yokoya, T. Nakamura, T. Matsushita, T. Muro, Y. Takano, M. Nagao, T. Takenouchi, H. Kawarada, and T. Oguchi, *Nature (London)* **438**, 647 (2005).

<sup>18</sup>G. Kresse and J. Furthmüller, *Comput. Mater. Sci.* **6**, 15 (1996).

<sup>19</sup>G. Kresse and D. Joubert, *Phys. Rev. B* **59**, 1758 (1999).

<sup>20</sup>R. F. Zhang, S. H. Sheng, and S. Veprek, *Appl. Phys. Lett.* **90**, 191903 (2007); **91**, 031906 (2007).

<sup>21</sup>R. F. Zhang, S. Veprek, and A. S. Argon, *Phys. Rev. B* **77**, 172103 (2008); *Appl. Phys. Lett.* **91**, 201914 (2007).

<sup>22</sup>N. N. Greenwood and A. Earnshaw, *Chemistry of Elements* (Pergamon Press, Oxford, 1984), Sec. 2.3.1, Fig. 2.4.

<sup>23</sup>R. F. Zhang, A. S. Argon, and S. Veprek, *Phys. Rev. Lett.* **102**, 015503 (2009); *Phys. Rev. B* **79**, 245426 (2009).